Effect of Additives on Mn/SiO₂ Based Catalysts on Oxidative Coupling of Methane

Mahmoodi, Somayeh; Ehsani, Mohammad Reza*+

Faculty of Chemical Engineering, Isfahan University of Technology, P.O. Box 84156-83111 Isfahan, I.R. IRAN

Hamidzadeh, Marzieh

Catalyst Department, National Petrochemical Company, Research & Technology (NPC-RT), Tehran, I.R. IRAN

ABSTRACT: *The Oxidative Coupling of Methane (OCM) over M-Na-Mn/SiO₂ catalysts (M=W, Cr, Nb and V) was investigated using a continuous-flow quartz reactor at 775°C, 1 atm and 100 $cm^3 min^{-1}$ gas flow rates, and correlated with the observed structure and redox properties. The interaction effects of the metal-metal and metal-support on the methane conversion and C_{2+} yield were investigated using X-Ray Diffraction (XRD), laser Raman spectroscopy, Fourier Transform Infrared Spectroscopy (FT-IR), and Temperature Programmed Reduction with H_2 (TPR). The results revealed that the improvement of C_{2+} selectivity (or C_{2+} yield) follows the order W>Cr>Nb>V, while the catalytic conversion did not change significantly. XRD data indicated that Mn is well dispersed on the SiO₂ support and also show that Mn_2O_3 and α-cristobalite were the predominant species in the surface catalysts. TPR data show that most of the Mn is present as Mn^{3+} and Mn^{2+}. FT-IR analyses combined with the Raman results show that terminal M=O and bridging M–O–M species and the metal–metal and metal–support interactions, which take place due to the presence of sodium ion, depend on the transition metal that affect the catalyst performance. Results reveal that the interaction between metal oxide and sodium is required for high selectivity and control redox mechanism in transition metal oxide in OCM reaction.*

KEY WORDS: *Oxidative Coupling of Methane (OCM), Structural properties, Transition metal oxide, Redox mechanism.*

INTRODUCTION

The Oxidative Coupling of Methane (OCM) to C_{2+} hydrocarbons has been intensively studied since 1980s, as one of the important potential routes to a possible future production of basic chemicals and liquid fuels from natural gas [1]. A large number of catalyst systems have so far been found to be effective in OCM. The Na_2WO_4-Mn/SiO₂ catalyst system, that identified by *Fang et al.*[1] as a promising catalyst, has attracted great attention because of its excellent catalytic performance.

The reaction mechanism of OCM is very complicated. The primary and most important step in this reaction is the hemolytic abstraction of hydrogen from the methane molecule by oxygen to produce a methyl radical that combines in the gas phase with another methyl radical or

29

hydrocarbon, yielding higher hydrocarbons. Mechanistic studies have identified two possible active oxygen species, namely: (i) molecular species such as, O_2^{2-} for lanthanide oxides, and (ii) dissociated oxygen species such as nucleophilic ions O^- of the catalyst lattice [1]. There are considerable controversies concerning on the nature of the active centre in the catalyst exist. For example in the case of $Mn/Na_2WO_4/SiO_2$, many researchers studied and have noticeable disagreement in the active sites on this catalyst. *Fang et al.* [1] Proposed a surface W species containing W=O and three W–O–Si bonds as the OCM active site, with manganese oxide enhancing the exchange between gaseous and lattice oxygen. This model was further developed by *Kou et al.* [2] With emphasis on the combination of tetrahedral WO_4 and octahedral MnO_6 sites, respectively responsible for the activation of methane and the lattice oxygen transport. The same catalyst was studied by *Lunsford et al.* [3]. suggested that a Na–O–Mn species was mainly responsible for the activation of methane, and that sodium was responsible for preventing the complete oxidation of CH_4. The presence of tungstate ions appears to impart stability to the catalyst. Recently, *Ji et al.* [4] proposed that both Na-O-Mn and Na-O-W species acted as the active sites of the catalyst. These conflicting results tempted us to clarify the nature of the active sites on the catalysts, which will be relevant to the rational design of new catalysts more efficient for the synthesis of C_2 hydrocarbons from the OCM reaction. In this study, a series of M–Na–Mn/SiO$_2$ catalysts (M=W, Cr, Nb and V) have been prepared with the same molar content as a 4.5% M – 9% Na – 2.8% Mn/SiO$_2$ catalyst and their catalytic performances for OCM were evaluated using a continuous-flow fixed-bed reactor. Characterization of M/Na/Mn/SiO$_2$ (M= W, V, Cr, Nb) from X-Ray Diffraction UV-vis spectroscopy, FTIR spectroscopy, TPR and Raman spectroscopy has been carried out to evidence effects following the promoter nature. Here, we report the significant effects of sodium salts containing different oxo anions on the structures and catalytic behaviors of the Mn/SiO$_2$-based catalysts. The oxo anions include Na_2WO_4, Nb_2O_5, $NaVO_3$, $Cr(NO_3)_3$ and $NaNo_3$. The effects of this wide variety of oxo anions have not been rigorously examined in the literature. The roles the various catalyst components were established by correlating the catalytic results with both bulk and surface

properties of the catalyst. The effect of the wide variety of oxo anions (V, Cr, Nb) will provide deep insight into the role of WO_4^{2-} and the active site requirements in the OCM reaction.

EXPERIMENTAL SECTION
Catalyst preparation
The M/Mn/SiO$_2$ catalysts were prepared by incipient wetness impregnation method. The silica gel support was first impregnated with an aqueous solutions containing an appropriate amount of $Mn(NO_3)_2$ and then various sodium salts. The sodium salts used in this work included Na_2WO_4, Nb_2O_5, $NaVO_3$, $Cr(NO_3)_3$ and $NaNo_3$. Samples were dried for 8h at $130^{\circ}C$ after impregnation and then calcined in air for 8h at 850 °C. All of dried catalyst samples were crushed and sieved to 25/35 mesh size. Herein, the amounts of the various components are expressed in same molar weight as 4.5% M - 9% Na - 2.8% Mn/SiO$_2$ catalyst (M=W, Cr, Nb and V). The catalysts were tested for 5 h and then unloaded. During the unloading, the reactor was allowed to cool to room temperature under a flowing N_2 atmosphere and then exposed to air before collection.

Catalytic activity test
The catalytic reaction was carried out in a tubular fixed bed quartz micro reactor (9 mm i.d.) located in a furnace. About 1.8 g catalysts were loaded in the reactor and the remaining volume was filled with quartz chips so as to minimize the contribution from any gas-phase reactions and preheat the gas in precatalytic section. The reactor was heated by an electrical furnace and a thermocouple was attached to the outside wall of the reactor to monitor the reactor temperature and to control the furnace. . Reactant gases which included CH_4 (99.9%), O_2 (99.95%) and N_2 (99.999% purity), were used at a ratio of 2:1:2. Gas flow rates were regulated with mass flow controllers. The catalysts were evaluated at 775ºC and 1 bar pressure with a GHSV of 8963 mlg^{-1}h^{-1}. These experimental conditions were applied to all activity tests. At the reactor outlet a cold trap was used to remove the water from the exit gas stream The reaction products were then analyzed with an on-line gas chromatography (HP Agilent 6890 N) equipped with TCD and FID, using a Porapak Q column for the separation of CH_4, CO_2, C_2H_4, C_2H_6, C_3H_6, and C_3H_8

Table 1: The Catalytic Performance of The M–W–Mn/SiO₂ Catalysts [a].

Catalyst	CH₄ Conversion	C₂ Selectivity	$\dfrac{C_2H_4}{C_2H_6}$	C₂ Yield	Gap Energy [b] (Ev)
Na-W–Mn/SiO₂	42.3	36.5	2.6	15.46	3.31
Na-Nb–Mn/SiO₂	41.3	14.6	4.3	6	4.52
Na-V–Mn/SiO₂	40.6	9.3	4.58	3.7	-
Na-Cr–Mn/SiO₂	37	19.4	2.2	7.2	2.29

[a] Reaction conditions: T=775°C; CH₄:O₂:N₂=2:1:2; GHSV=8963 mlg⁻¹h⁻¹; 1.8 g catalyst; stream time = 2.5 h.

[b] Gap energy were identified by UV-vis spectroscopy according to the follow equation: Gap energy=(1239/ maximum wave length).
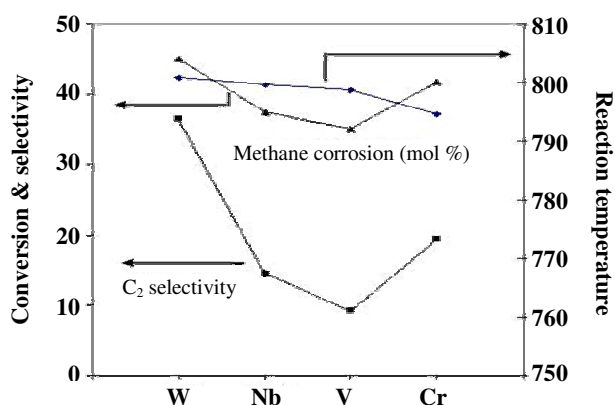
Fig. 1: OCM catalytic performance of M/Na/M/SiO₂ catalysts.

and a 5 Å molecular sieve column for the separation of O₂, CH₄, and CO.

Catalyst characterization

X-ray diffraction (XRD, Phillips diffractometer) was used to characterize the crystal structures of the synthesis catalysts. FTIR spectra of samples were recorded with shimadzue 8400 FTIR spectrophotometer using KBr palate at 25°C in the range 400 to 4000 cm⁻¹. Raman spectra were recorded in a thermo Nicolet dispersive Raman spectrometer. The resolution was 4 cm⁻¹. Raman shifts for all the samples were measured in the range 400-1200 cm⁻¹. UV-vis diffuse reflectance spectra were done on a shimadzue 2500 spectrophotometer. Temperature-Programmed Reduction (TPR) measurements were performed in a flow unit (Micromeritics plus Chemisorb 2705) equipped with a TCD detector. Samples (100 mg, calcined at 623 K in N₂) were placed in a quartz cell and heated linearly from 293 to 1323 K at 10 K min⁻¹ in flowing 6% H₂/Ar (45 cm³ min⁻¹).

RESULTS

Catalytic reaction results

Table 1 shows the effects of different promoters on the C₂ selectivity and methane conversion over M-Na-Mn/SiO₂ catalysts (M= W, Nb, Cr, and V). The results in table 1 indicate that the addition of W is most effective in improving the yield of catalyst. The addition of V, Cr or Nb leads to decrease in selectivity to C₂ hydrocarbons. As indicated in Fig. 1, sodium salts, specifically the corresponding oxo anions, largely affected on C₂ selectivity. The results indicated that the catalysts showed almost the same catalytic conversion in OCM reaction. It should be noted that, the OCM reaction, and more so far the deep oxidation reactions, is very exothermic. The reactor temperature will increase with the accumulation of reaction heat and hot spots will be present in the catalyst bed. The exothermic reactions that occur during the oxidative coupling of methane over catalysts result in relatively narrow hot spots that may produce temperature increases as large as 40°C.

X-ray diffraction

In order to obtain information about the principle components of catalysts, X-Ray Diffraction (XRD) was used to identify bulk phase composition and crystal size in different catalysts. The XRD patterns of catalysts are shown in Fig. 2. It can be seen that the main crystallite phases of catalysts were Mn₂O₃ and α-cristobalite. Thus the initially amorphous silica underwent complete conversion to highly crystalline α-cristobalite during calcination in presence of the Na⁺ ion, as a structural promoter, at a temperature far below the normal transition temperature of 1500°C [5], except that a little of quartz were detected in Nb catalyst. It was also observed that significant

Table 2: Phase identification and crystal size of the M/Na/Mn/SiO$_2$ catalysts.

| Catalysts[a]	Formula	Crystallite phase	Size(nm)	Formula	Crystallite phase	Size(nm)
W/Na//Mn/SiO$_2$	SiO$_2$	Cristobalite, syn	29.9	Na$_2$WO$_4$	Sodium Tungsten Oxide	28.5
	SiO$_2$	Tridymite	29.9	Mn$_2$O$_3$	Bixbyite-C, syn	38.4
Nb/Na//Mn/SiO$_2$	SiO$_2$	Cristobalite, syn	30.9	Mn$_2$O$_3$	Bixbyite-C, syn	35.0
	SiO$_2$	Quartz, syn	46.8			
V/Na//Mn/SiO$_2$	SiO$_2$	Cristobalite, syn	40.5	Mn$_2$V$_2$O$_7$	Manganese Vanadium Oxide	7.8
	Mn$_2$O$_3$	Bixbyite-C, syn	30.5			
Cr/Na//Mn/SiO$_2$	SiO$_2$	Cristobalite, syn	23.8	Mn$_2$O$_3$	Bixbyite-C, syn	20.3
	MnO	Manganosite	18.7			

[a] *The crystalline phase were identified by XRD and the size of crystal was calculated according to the Scherrer equation:* $d = \frac{\lambda_{max} K}{\beta . \cos\theta}$
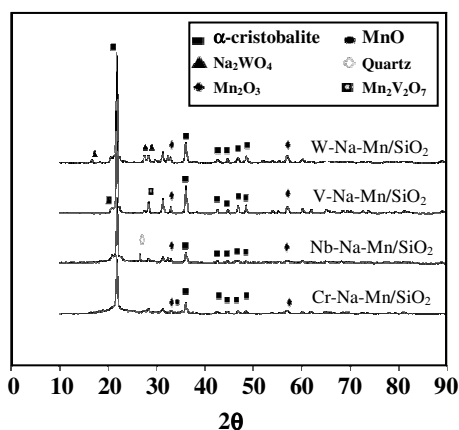
Fig. 2: XRD patterns of M/Na/Mn/SiO$_2$ catalysts.

amounts of crystalline phases of Na$_2$WO$_4$ were present on the W catalyst, which shows Na has a higher affinity to combine with WO$_4$ than with Mn. In V catalyst the Mn$_2$V$_2$O$_7$ phase indicates affinity between Mn and V. Niobium oxide and chromium oxide is not observed in the XRD patterns of Nb-Na–Mn/SiO$_2$ and Cr-Na-Mn/SiO$_2$ catalysts, respectively. Therefore, Mn is converted into Mn$_2$O$_3$ and MnO phases in these catalysts.

Table 2 shows the phase composition and crystal size of the different catalysts. The comparison with catalyst performance shows that the crystal size of the α-cristobalite and Mn$_2$O$_3$ does not exert a significant effect on the catalyst performance. According *Tanabe et al.* [6] research is provided strong evidence that the reversible activation of methane on OCM catalysts is initiated by the hetrolytic abstraction of an H$^+$ on the basic sites O^{2-} (alkaline metal oxide sites) of the surface, the remaining

methyl anion CH$_3^-$ being linked to the surface cations M^{n+}. It is assumed that the anionic species CH$_3^-$ produced by the reversible activation of methane on anion/cation pairs of the oxide surface may react with an electron acceptor to form a methyl radical as follow:

$$CH_3^- = CH_3^0 + e^-$$
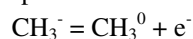
On reducible oxides such as W in Na$_2$WO$_4$ structure is created an electron donor-acceptor site. This contribution site can act as ellectrophilic species and abstract the electron from CH$_3^-$. The other synthetic catalysts can not provide this synergic effect. Therefore, Na$_2$WO$_4$ /Mn/SiO$_2$ catalyst has the best selectivity on OCM reaction.

Laser Raman spectroscopy

Fig. 3 shows the Raman spectra of catalysts in the range 400-1200 cm^{-1}. By comparing Fig. 3 with literature results, one can assign the Raman bands between 700-500 cm^{-1} can be ascribed to manganese oxide species and those below 500 cm^{-1} to α-cristobalite and quartz[4]. The band at 695 cm^{-1} may correspond to the stretching modes of the Mn–O lattice[7] in Mn$_2$O$_3$. This bond shifts to lower wave number 688 and 694 cm^{-1} in W and V catalysts, and shifts to higher wave number 697 cm^{-1} in Cr catalyst. The Raman bands of Mn$_2$O$_3$ were detected on the catalysts containing W at 688, V at 584, 694, Cr at 553, 575, 605, 697, and Nb at 579 cm^{-1}. On V-Na-Mn/SiO$_2$ catalyst the broad bands observed between 820 and 920 cm^{-1} with maximum at about 870 cm^{-1} correspond to V–O stretching modes[8]. The V=O, Cr=O and W=O stretching modes are near 1021, 1019 and 1019 cm^{-1}, respectively [9]. Comparison with the literature results
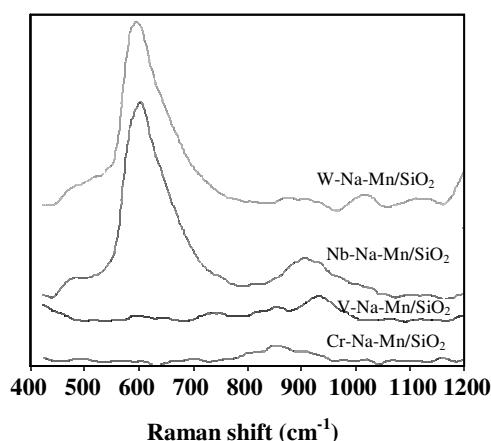
Fig. 3: Raman spectra for catalysts.

Fig. 4: FT-IR spectra for catalysts.

suggests that the Raman bands between 952 and 905 cm^{-1} can be assigned to tetrahedral WO_4, and bands between 889 and 862 cm^{-1} to octahedral WO_6[4]. In W-Na-Mn/SiO₂ catalyst the band at 882 cm^{-1} may be assigned to octahedral WO_6.

FTIR spectroscopy

The FTIR spectra of the M-Na-Mn/SiO₂ catalysts are shown in Fig. 4. The IR bands of the α-cristobalite are at 1200, 1092, 793, 619, and 483 cm^{-1} [10] that band at 1100 cm^{-1} relative to the shoulder at 1200 cm^{-1} could be owing to a superimposing of a Mn-O-Si vibration that arises from the bi-dimensional layer at the interface between SiO_2 and Mn_2O_3 [11]. The IR spectra of the α-cristobalite for the different catalysts) are as follows:

Na–W-Mn/SiO₂: 1200, 1097, 796, 622, 489 cm^{-1}

Na–Nb-Mn/SiO₂: 1167, 1099, 792 cm^{-1}

Na–V-Mn/SiO₂: 1198, 1093, 794, 622 cm^{-1}

Na–Cr-Mn/SiO₂: 1201, 1099, 795, 621, 470 cm^{-1}

Comparison the IR bands of catalysts with the α-cristobalite reveal that the presence of sodium salts brings about a change in the IR bands of the α-cristobalite. This indicates a close interaction of the sodium salts with α-cristobalite. The IR bands of the amorphous SiO_2 are at 1101, 971, 801, and 466 cm^{-1} [10]. In the Na–W-Mn/SiO₂ catalyst, this is at 971 cm^{-1}. Based on the FT-IR reported in the literature [12] the band at 960 cm^{-1} is due to a Si-O vibration mode perturbed by the presence of metal ions in a neighboring position. A comparison with the catalysts shows that this bond shifts to lower wave number (936 cm^{-1} and 958 cm^{-1}) in the Na–Nb-Mn/SiO₂ and Na–V-Mn/SiO₂ catalysts
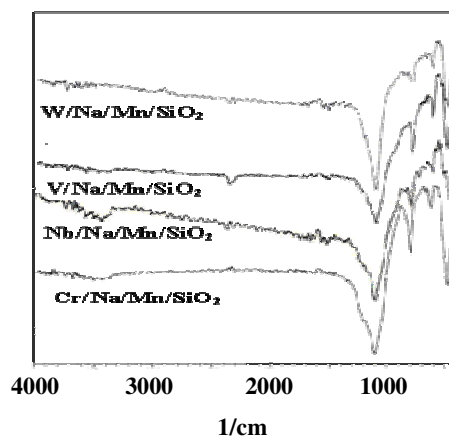
respectively, and in the Na-W-Mn/SiO₂ catalysts appear at 929 and 971 cm^{-1}. FTIR spectrum, shows no absorption near 635,903,948 cm^{-1} associated with V-O vibration[13] and near 1045, 2050 and 1027 cm^{-1} associated with V=O vibration and V=O stretching bond respectively belonging to vanadium oxide[14]. It seems that the IR bands of the sodium salts and manganese oxide species in the catalysts cannot be separated, although the IR bands of α-cristobalite, amorphous SiO_2, and quartz SiO_2 are distinguishable. The spectra of W, V and Cr catalysts exhibit a broad absorption band in the 3750–3500 cm^{-1} region due to the surface hydroxyl groups[14].

Temperature-Programmed Reduction (TPR)

Temperature Programmed Reduction (TPR) patterns of catalysts are shown in Fig. 5.

TPR pattern of catalyst shows broad reduction pattern in the range of 550–787°C, with peak at 610°C for W, V and Cr, correlates with Mn species with the reduction of Mn^{3+} to Mn^{2+} [15]. The W/Na/Mn/SiO₂ catalyst shows two peaks at 610 and 855°C that correlate with reduction of manganese oxide and wolfram oxide species, respectively [15], and a shoulder at 415°C corresponding to the reduction of Mn_2O_3 [16]. In Nb/Na/Mn/SiO₂ catalyst a broad peak with a maximum at 657°C could be due to the reduction of niobium species [17] that this phase is not observed in the XRD pattern.

DISCUSSION

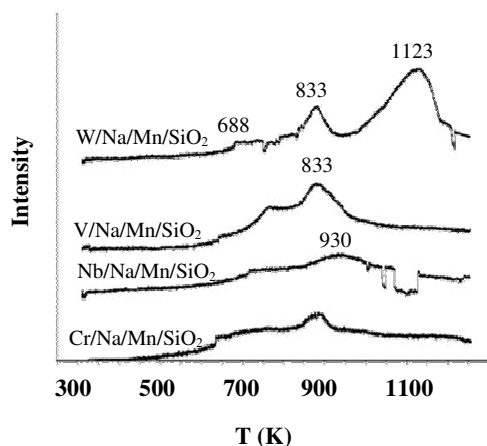The structural properties of the Mn/SiO₂-based catalysts and their catalytic performances in the OCM reaction largely

Fig. 5: TPR profiles of catalysts.

depend on the sodium salt added (i.e., both the Na^+ ions and oxo anions). As indicated from the results of Table 1, the improvement of C_{2+} selectivity (or C_{2+} yield) follows the order W> Cr>Nb>V. The role of sodium ions, which dominate the near-surface region of catalyst, may be to disperse the Mn ions. Na^+ is known to be a required component of the Mn/SiO_2-based catalysts, particularly for achieving the good C_2 selectivity in the OCM reaction. The promoting role of the Na^+ ions was previously attributed to their beneficial effects on the transformation of amorphous SiO_2 to α-cristobalite and the enhancement of the surface basicity [3]. It is known that basic surfaces tend to interact more weakly than acidic surfaces with C_2H_4, thus favoring desorption of C_2H_4 to reduce its combustion and increase its selectivity. Amorphous SiO_2 indeed catalyzed the combustion of C_2 products while α-cristobalite was inert in the OCM reaction. These previous findings are consistent with our results; addition of the sodium salts to Mn/SiO_2, irrespective of the identity of their anions, led to exclusive transformation of amorphous SiO_2 to α-cristobalite (Fig. 2) Na-O-M sites are created only on Na-Mn-W/SiO_2 catalyst and these sites act as the electron donor - acceptor sites and promote C_2 selectivity in this catalyst.

The reaction mechanism of OCM is very complicated and considerable controversies concerning the nature of the active centre in the catalyst exist. OCM process involves both the heterogeneous (surface catalyses) and homogeneous (gas phase) reactions. *Sofranko et al.* [18], suggested that the mechanism of the OCM process over

the catalyst of manganese oxide on silica involved an abstraction of H-atom from methane to form methyl radicals, this was the most important step in the whole conversion-activation of methane, and then two methyl radicals dimerized in the gas phase to produce ethane, while ethylene was from the oxidative dehydrogenation of ethane. It was well known that the formation of methyl radicals over the metal oxide catalysts was via the interaction of methane with the surface-active oxygen species, while the transports of gas phase oxygen to surface oxygen ions, maybe O^{2-}, O_2^- or O_2^{2-}, over surface catalytic site might be the key step of the formation of active oxygen species [19].
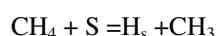
$CH_4 + S = H_s + CH_3$
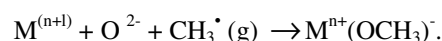Surface on catalyst- heterogeneous reaction
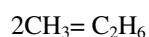
$2CH_3 = C_2H_6$
gas phase- homogeneous reaction

Lunsford [20] and co-workers suggested that the reaction of $CH_3^•$ radicals with a metal oxide may occur through electron transfer to the metal ion with the concomitant formation of a methoxide ion:

$$M^{(n+l)} + O^{2-} + CH_3^• (g) \rightarrow M^{n+}(OCH_3)^-.$$

A redox mechanism is proposed for the selective oxidation of methane to methyl radical. According to this mechanism, the active oxygen species was surface lattice oxygen O_s^{2-}. In the W catalyst, methane activation takes place on the W^{6+} sites, while activation of gas-phase oxygen occurs on the Mn^{3+} sites. CH_4 was activated by O_s^{2-} to generate $CH_3^•$ radical on $W^{6+/5+}$ site, and the electron transferred from $W^{6+/5+}$ site to $Mn^{3+/2+}$ site, which was responsible for molecular oxygen activation to form surface lattice oxygen O_s^{2-} as an active oxygen species for CH_4 activation.

These observed effects of sodium and oxo-anions on the formation of the active sites and the catalytic performance provide new insights into the understanding of the Mn/SiO_2-based catalysts and will be helpful for the synthesis of more efficient OCM catalysts.

CONCLUSIONS

Sodium salts and different oxo anions largely influence the structures, reducibility, and catalytic performances of the Na-M-Mn/SiO_2 based catalysts in the oxidative coupling of methane reaction. Here M is

Archive of SID

V, Cr, Nb, and W. Among these catalysts, Na_2WO_4-Mn/SiO₂shows the best catalytic performance at the OCM reaction conditions. Selective oxidation is provided by terminal M=O and bridging M–O–M species called also lattice oxygen bonded and support–metal and metal-metal interactions having nucleophilic nature. Catalysts crystallization critically depends on the presence of the sodium ion, which is accompanied with different metal-metal and metal–support interactions. In agreement with XRD and TPR results disappeared interaction between Nb and Cr oxides and silica support in Na-Nb-Mn/SiO₂ and Na-Cr-Mn/SiO₂ catalysts produced poor catalyst. Higher selectivity, which is related to different interactions in catalysts, however, is observed in catalyst containing W oxide compared to catalysts containing Nb and Cr metal oxides. Results express that the interaction between metal oxide and sodium is required for high selectivity and control redox mechanism in transition metal oxide in OCM reaction. Clearly, more mechanistic studies are needed in this field, especially related to identification of various oxygen species on the catalyst surface and their possible role in the oxidation.

REFERENCES

[1] Fang X.L.S.L. J., Gu J., Yang D., Preparation and Characterization of W-Mn Catalyst for Oxidative Coupling of Methane. *Chin. J. Mol. Catal.*, **6**, p. 255 (1992).

[2] Kou Y. et al., Amorphous Features of Working Catalysts: XAFS and XPS Characterization of Mn/Na₂WO₄/SiO₂ as Used for the Oxidative Coupling of Methane, *Journal of Catalysis*, **173**, p. 399 (1998).

[3] Dingjun Wang, M.P.R., Jack H. Lunsford, Oxidative Coupling of Methane over Oxide-Supported Sodium-Manganese Catalysts, *Journal of Catalysis*, **155**, p. 390 (1995).

[4] Sheng-fu Ji, T.-c.X., Shu-ben Li, Chuan-zhi Xu, Rui-ling Hou, Karl S. Coleman, Malcolm L.H. Green, The Relationship Between the Structure and the Performance of Na-W-Mn/SiO₂ Catalysts for the Oxidative Coupling of Methane, *Applied Catalysis A: General*, **225**, p. 271 (2002).

[5] Alejandra Palermo J.P.H.V., Adam F. Lee, Mintcho S. Tikhov, Richard M. Lambert, Critical Influence of the Amorphous Silica-to-Cristobalite Phase Transition on the Performance of Mn/Na₂WO₄/SiO₂ Catalysts for the Oxidative Coupling of Methane. *Journal of Catalysis*, **177**, p. 259 (1998).

[6] Utiyama M., Hattori H., Tanabe K., Exchange Reaction of Methane with Deuterium over Solid Base Catalysts, *Journal of Catalysis*, **53**, p. 273 (1987).

[7] Effendi Widjaja J.T.S., Xuan Ding Han, Eunice Goh, Use of Raman Microscopy and Band-Target Entropy Minimization Technique to Differentiate Physical Mixture from Chemical Mixture in Mixed Metal Oxides, *Catalysis Today*, **131**, p. 21 (2008).

[8] A. Klisin´ska S.L., Grzybowska B., Stoch a J., Gressel I., Effect of Additives on Properties of V₂O₅/SiO₂ and V₂O₅/MgO Catalysts II. Structure and Physicochemical Properties of the Catalysts and Their Correlations with Oxidative Dehydrogenation of Propane and Ethane, *Applied Catalysis A: General*, **309**, p. 17 (2006).

[9] M.O. Guerrero-Pe´rez, M.C.H., I. Malpartida , M.A. Larrubia , L.J. Alemany , M.A. Ban˜ares, Operando Raman Study of Propane Oxidation over Alumina-Supported V-Mo-W–O Catalysts, *Catalysis Today*, **126**, p. 177 (2007).

[10] Shengfu Ji, T.X., Shuben Li, Lingjun Chou, Bing Zhang, Chuanzhi Xu, Ruiling Hou, Andrew P.E. York, Malcolm L.H. Green, Surface WO₄ Tetrahedron: the Essence of the Oxidative Coupling of Methane over M–W–Mn/SiO₂ Catalysts, *Journal of Catalysis*, **220**, p. 47 2003.

[11] Florina Buciuman, F.P., Radu Craciun, Dietrich R.T. Zahn, Vibrational Spectroscopy of Bulk and Supported Manganese Oxides, *Phys. Chem. Chem. Phys.*, **1**, p. 185 (1999).

[12] Maria Ziolek, I.S., Anna Lewandowska, Izabela Nowak, Piotr Decyk, Monika Renn, Beata Jankowska, Oxidative Properties of Niobium-Containing Mesoporous Silica Catalysts Catalysis Today, **70**, p. 169 (2001).

[13] Arthur Dobley, K.N., Shoufeng Yang, Peter Y. Zavalij, M. Stanley Whittingham, Manganese Vanadium Oxide Nanotubes: Synthesis, *Characterization, and Electrochemistry. Chem. Mater.*, **13**, p. 4382 (2001).

[14] Carlo Resini, T.M., Guido Busca, Jih-Mirn Jehng, Israel E. Wachs, Comparison of Alcohol and Alkane Oxidative Dehydrogenation Reactions over Supported Vanadium Oxide Catalysts: in Situ Infrared, Raman and UV–Vis Spectroscopic Studies of Surface Alkoxide Intermediates and of Their Surface Chemistry, *Catalysis Today*, **99**, p. 105 (2005).

[15] A. Malekzadeh, A.K., A. K. Dalai, M. Abedini, Oxidative Coupling of Methane over Lithium Doped (Mn+W)/SiO$_2$ Catalysts, *Journal of Natural Gas Chemistry*, **16**, p. 121 (2007).

[16] E.R. Stobbe, B.A.d.B., J.W. Geus, The Reduction and Oxidation Behaviour of Manganese Oxides, *Catalysis Today*, **47**, p. 161 (1999).

[17] Maria Ziolek, I.S., Anna Lewandowska, Izabela Nowak, Piotr Decyk, Monika Renn, Beata Jankowska, Oxidative properties of Niobium-Containing Mesoporous Silica Catalysts, *Catalysis Today*, **70**, p. 169 (2001).

[18] Sofranko J.A., Leonard J.J., Jones C.A., Gaffney A.M., Withers H.P., Catalytic Oxidative Coupling of Methane over Sodium-Promoted Mn/SiO$_2$ and Mn/MgO, *Catalysis Today*, **3**, p. 127 (1988).

[19] Yu Z. Q., Y.X.M., Lunsford J. H., Rosynek M. P., Oxidative Coupling of Methane over Na$_2$WO$_4$/CeO$_2$ and Related Catalysts, *Journal of Catalysis*, **154**, p. 163 (1995).

[20] Lunsford J.H., A Study of Catalysts and Mechanisms in Synthesis Ractions, Texas A&M University, (1991).